

Cocoid-Like Microstructures in a 3.0 Ga Chert from Western Australia

YUICHIRO UENO,¹

*Research Center for the Evolving Earth and Planets, Department of Environmental Science and Technology,
Tokyo Institute of Technology, Post No. S2-17, Midori-ku, Yokohama 226-8503, Japan*

YUKIO ISOZAKI,

Department of Earth Science and Astronomy, University of Tokyo, Meguro, Tokyo 153-8902, Japan

AND KENNETH J. MCNAMARA

Department of Earth and Planetary Sciences, Western Australia Museum, Perth, WA 6000, Australia

Abstract

Organic-walled spheroidal microstructures were discovered in a 3.0 Ga chert of the Cleaverville Formation, Western Australia. The spheroids are composed of solitary or paired cell-like units enclosed by an outer envelope, which are apparently similar to cyanobacterial microfossils. However, some of the spheroidal structures appear to be related to the arrangement of the surrounding minerals, and some to overprint diagenetic fabrics. Despite several cell-like characteristics, such as organic composition, paired nature, and multi-layered envelopes, at least some spheroids were formed during diagenesis, and thus are of diagenetic origin rather than being fossilized cells. It has been generally difficult to distinguish Archean microfossils from abiotic carbonaceous structures, however, and such microscopic observations could demonstrate the abiotic origin of some superficially fossil-like structures produced during diagenesis.

Introduction

MORPHOLOGICALLY PRESERVED ARCHEAN microfossils are direct evidence for the existence of life on the early Earth (e.g., Altermann and Kazmierczak, 2003). The putative microfossils so far have been reported from Archean strata, such as the 3.5–3.0 Ga Pilbara Supergroup, Australia (Awramik et al., 1983; Schopf, 1993; Rasmussen, 2000; Ueno et al., 2001) and the penecontemporaneous Swaziland Supergroup, South Africa (Knoll and Barghoorn, 1977; Walsh and Lowe, 1985; Westall et al., 2001). They show filamentous and coccoidal morphologies, some of which resemble cyanobacteria (Awramik et al., 1983; Schopf, 1993). In contrast to well-preserved microfossils in younger Proterozoic strata, the biological origins of some Archean microfossils are still a matter of debate (e.g., Brasier et al., 2002; Schopf et al., 2002). Inorganic minerals coated by carbonaceous materials can possibly show prokaryote-like morphologies (Schopf and Oehler, 1976; Buick, 1990; Brasier et al., 2002; Garcia-Ruiz et al., 2003). It is not yet well established how to distin-

guish real microfossils from these abiologically produced fossil-like structures (Cady et al., 2003; Hofmann, 2004).

Here, we report new types of spheroidal carbonaceous structures in the 3.0 Ga chert from the Cleaverville Formation in the Pilbara craton, Western Australia (Fig. 1), which resemble coccoidal prokaryote. The purpose of this study is to document their mode of occurrence and morphological variations. Both biological and abiological interpretations are plausible for the origin of the structures. We further discuss the two possibilities in order to search for the criteria distinguishing authentic microfossils.

Cleaverville Formation

The Cleaverville Formation is composed of bedded chert, banded iron formation, siltstone, sandstone, and minor volcanoclastic rocks (Hickman et al., 2001). The unit overlies pillowed basaltic greenstone of the Regal Formation, and is unconformably overlain by the 2775 ± 10 Ma Mt. Roe Basalt (Hickman et al., 2001). The minimum depositional age of the Cleaverville Formation is constrained by a 3014

¹Corresponding author: email: ichiro@depe.titech.ac.jp

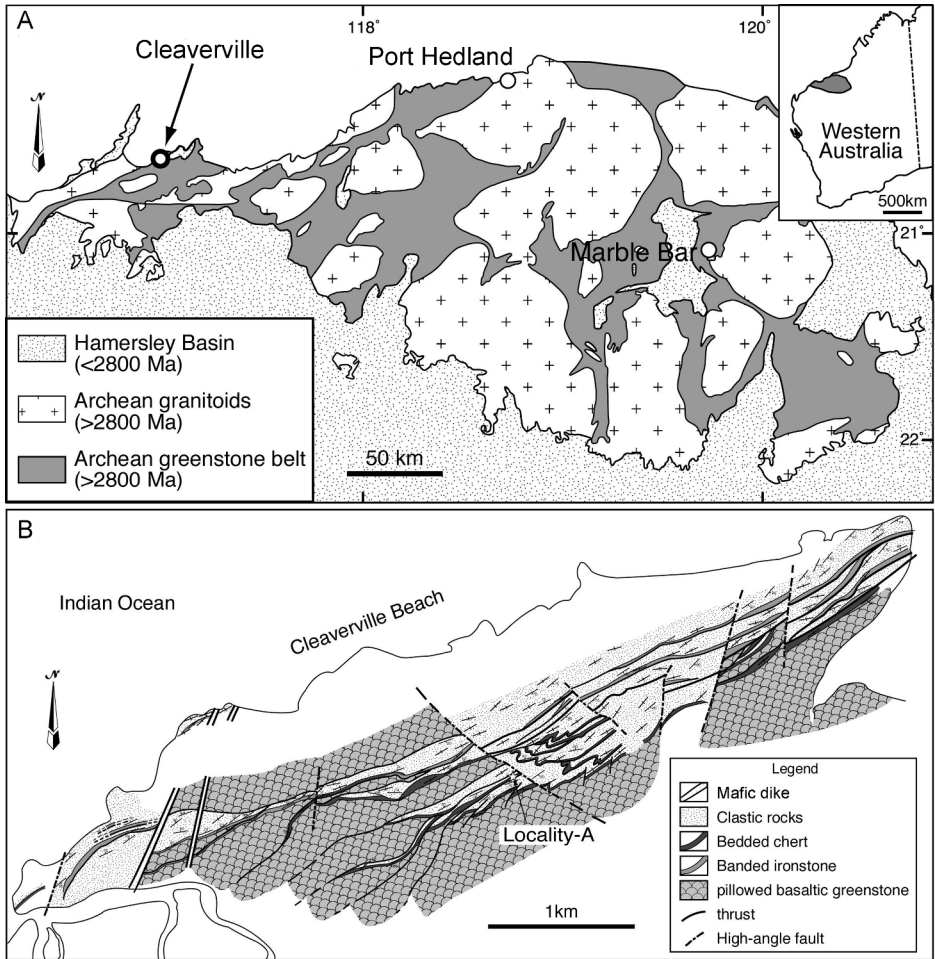


FIG. 1. A. Geological map of the Pilbara craton, Western Australia. B. Geological map of Cleaverville Beach, showing the sample locality (Locality A).

± 6 Ma intrusive granophyre, and a maximum age by the presence of 3018 ± 3 Ma detrital zircons in the volcanoclastic rock (Hickman et al., 2001). The metamorphic grade of the Cleaverville Formation including the rocks studied here is generally low (prehnite-pumpellyite to lowermost greenschist facies; Ohta et al., 1996; Hickman et al., 2001).

The depositional environment of the Cleaverville Formation is poorly understood and somewhat controversial. Three different tectonic settings have been proposed for the deposition of the chert and underlying pillow basalt, including: (1) mid-oceanic ridge (Ohta et al., 1996; Kato et al., 1998); (2) oceanic island arc (Kiyokawa and Taira, 1998); and

(3) continental margin (Hickman et al., 2001). The chert is mainly composed of fine-grained silica and shows massive or parallel lamination, although lacking both coarse-grained terrigenous clastics and wave-influenced sedimentary structures such as cross-lamination (Ohta et al., 1996; Kato et al., 1998). Their absence may suggest that chemical precipitation of silica was responsible for the formation of the chert. A positive Eu anomaly of the chert indicates that it was precipitated from silica-rich hydrothermal water (Kato et al., 1998). An anomalously low Al/Ti ratio of some Cleaverville cherts possibly resulted from either hydrothermal alteration or chemical weathering (Sugitani et al., 1996).

Samples and Methods

The spheroid-bearing black chert was collected from Cleaverville Beach (named Locality-A; UTM grid 2356-008149; Fig. 1). At this locality, a ~20 m thick black laminated chert bed overlies pillowed basaltic greenstone and is overlain in turn by siltstone. The greenstone/sedimentary rock sequence strikes NE-SW and dip steeply at ~70° to the north. Continuous outcrop of the chert can be traced laterally for ~500 m. In this outcrop, the black laminated chert is generally disturbed by secondary faults, often stained by Fe oxide, and partly folded, although the lowermost part of about 80 cm thickness is less deformed, showing continuous original lamination. We collected a relatively unaltered chert specimen (~2 kg) from the lowermost part.

The hand specimen of the black chert was first cut perpendicular to the bedding surface. Seven doubly polished thin sections were made to cover the entire cut surface. Sedimentological and micropaleontological observations were conducted under the microscope in transmitted and reflected light. In addition, a laser Raman microspectrophotometer was used for characterizing carbonaceous materials and inorganic minerals. Details for the Raman analysis are given elsewhere (Ueno et al., 2004).

More than 15,000 carbonaceous spheroids were identified in the seven thin sections. We focused on about 500 spheroids, which are relatively clear in shape and away from cracks and veins. The 3D morphologies of the 500 spheroids were described in detail, and then photographed individually for measuring their dimensions.

Lithology

The spheroid-bearing black laminated chert is mainly composed of an interlocking mosaic of microcrystalline quartz (<~10 µm) with disseminated black carbonaceous matter (kerogen) and minor amounts of fine-grained pyrite and carbonate (typically <5 µm). The chert contains no coarse-grained clastics or their remnants (Fig. 2). Detailed microscopic observations identified five distinctive sedimentary fabrics (i.e., F1 to F5; Fig. 2). Each fabric typically constitutes a 0.1–10 mm thick layer (Fig. 2A), although one fabric sometimes changes laterally into another (Fig. 2C).

F1 represents homogeneous fabric (Figs. 2A and 2B). The relatively clear color of the F1 texture is due to a low amount of disseminated kerogen. The

carbonaceous spheroids are sparsely distributed in F1.

F2 is composed of densely packed carbonaceous spheroids, which are aligned along the bedding surface and generally constitute a thin (~100 µm) layer (Figs. 2G and 2H). Some spheroids are elongated parallel to the bedding, indicating post-depositional compaction (Fig. 2G). The F2 layer is typically overlain by F3 (Fig. 2G), locally bounded by stylolites (Fig. 2H), where the aggregate of the spheroids is disturbed and broken. On the other hand, the bottom part of the F2 layer grades into the F1 in many cases.

F3 is characterized by a cloudy texture (Fig. 2F) with lesser amounts of the spheroids than in F2 and more common than in F1. Contrasts in kerogen concentrations are responsible for the grey to black cloudy appearance. The spheroids are randomly distributed, and some are attached to each other. The F3 layer typically overlies F2, whereas the top of the F3 layer is invariably bounded by secondary infiltrated silica (F4) with irregular boundaries.

F4 is a sill or lens, which apparently infilled pre-existing open space (Figs. 2A and 2D). F4 consists of chalcedony, now composed of microcrystalline quartz (Fig. 2D). The symmetric crystal growth pattern clearly indicates a secondary origin for F4. Irregular shaped, diffuse boundaries between the F4 and the other textures suggests that silica-rich fluid infiltrated before consolidation, probably during early diagenesis. No carbonaceous spheroids occur in F4.

F5 is a lenticular intralaminar structure (Figs. 2A, 2C, and 2E), which constitute a >1 cm thick layer. Billowy kerogen-rich thin layers surround kerogen-poor lenticular masses. Both the lenses and small kerogenous grains in F5 are generally elongated parallel to the bedding surface, suggesting compaction (Fig. 2E). Spheroids are rare in F5.

These fabrics are further overprinted by randomly oriented quartz veins (Figs. 2A, 2C, 2E, and 2F). In contrast to F4, they have sharp boundaries, and the quartz is coarse grained (>100 µm). Kerogen is absent from the veins.

In summary, silica-rich fluid infiltrated in more than two stages (i.e., the chalcedonic sill of F4 and later-stage quartz veins), and this may be responsible for silicification of the black chert. The late-stage quartz veins would have formed after compaction because they cut the compaction-related structures of F2 and F5. On the other hand, the chalcedonic sill of F4 may have formed during early

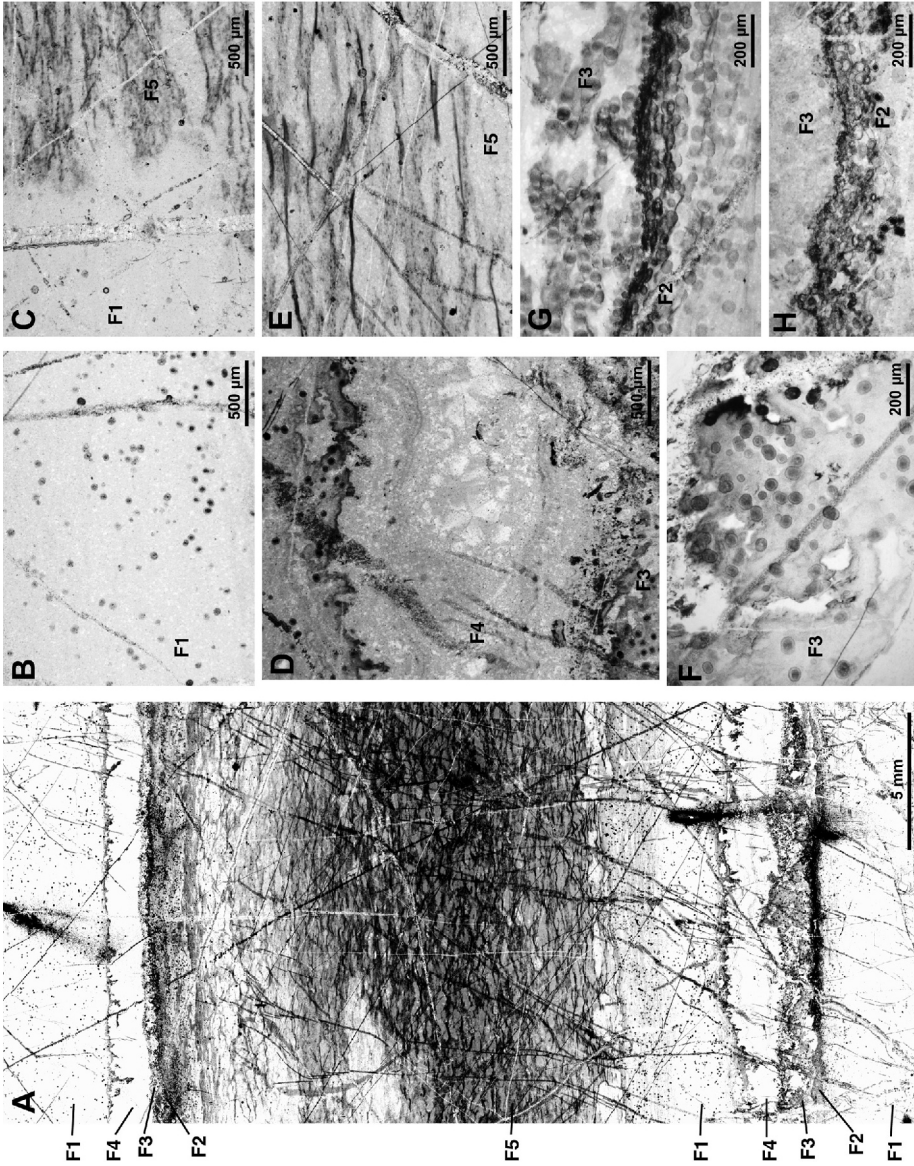


FIG. 2. Photomicrographs of the spheroid-bearing black laminated chert. All the figures show vertical cross-sections of the chert. Tops of the figures are stratigraphic tops. A. Photograph of a thin section. F1 to F5 indicate sedimentary fabrics. Remaining figures show magnified views of F1 (B and C), F2 (G and H), F3 (D, F, G, and H), F4 (D), and F5 (C and E). See text for details.

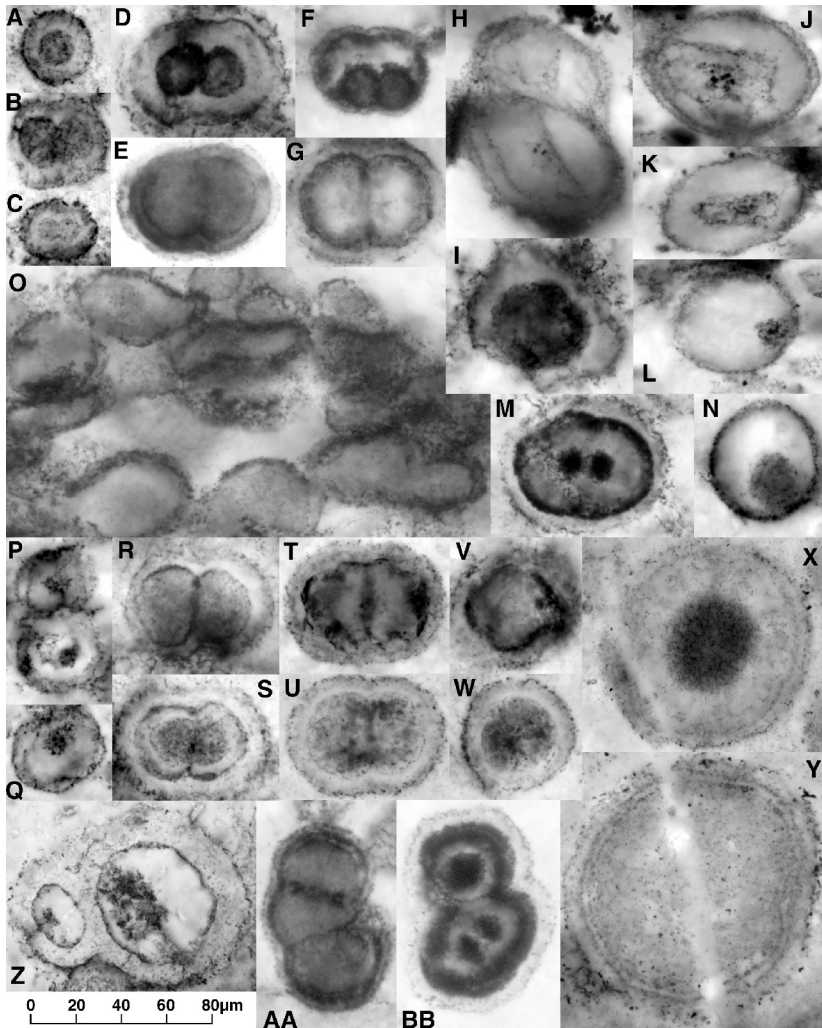


FIG. 3. Photomicrographs showing individual carbonaceous spheroids. A–C, P–Q. Small-sized spheroids. D–N, R–W, AA–BB. Large-sized populations. X–Z. Exceptionally large specimens. The scale at the bottom left represents 80 μm for all the figures.

diagenesis, possibly before compaction, because of the irregular-shaped boundary of F4 and others (Figs. 2A and 2D). The absence of coarse-grained clastic materials suggests that the chert was originally deposited as carbonaceous mud before silicification. However, direct precipitation of silica cannot be fully dismissed.

Carbonaceous Spheroids

The carbonaceous spheroids are coccoid-like microstructures that are composed of thin (<1 μm) organic walls (Fig. 3). Figure 4 shows their Raman

spectra, indicating carbonaceous compositions. Their three-dimensional structures are preserved in a microcrystalline quartz matrix (Fig. 5). Very fine carbonate particles (< 1 μm) occur along some spheroids (Figs. 4 and 5). Some spheroids are further replaced and/or coated by pyrite (Fig. 6E), and subsequently by Fe oxide (Fig. 6F). In these altered specimens, their thin organic walls are typically obscure.

The spheroids consist of solitary, or most commonly paired, cell-like units, which are generally enclosed by an outer envelope (Fig. 3). Among the 500 specimens observed, ~75% are paired, and the

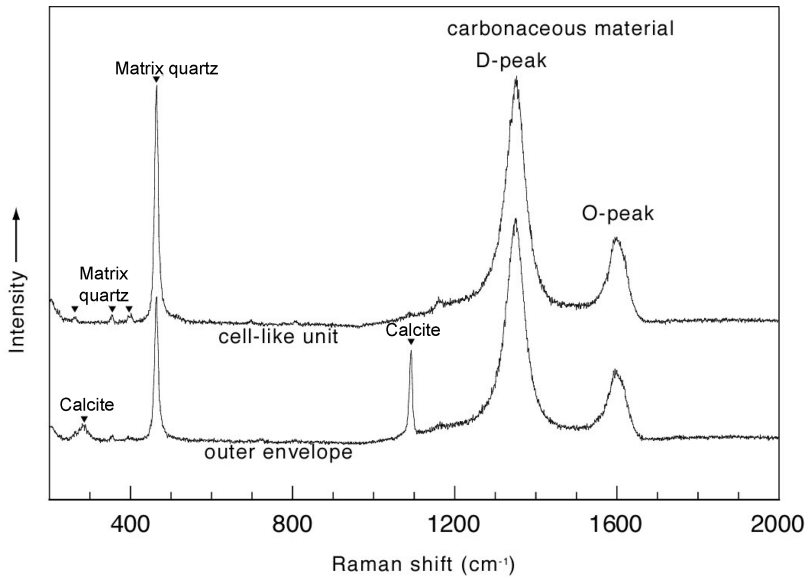


FIG. 4. Representative Raman spectra for the carbonaceous spheroids. O-peak (near 1600 cm^{-1}) and D-peak (near 1350 cm^{-1}) are from carbonaceous material. The microscope objective used is 100x; thus the analytical spot size is about $1\text{ }\mu\text{m}$. Details of the micro-Raman analytical procedure are given in Ueno et al. (2004).

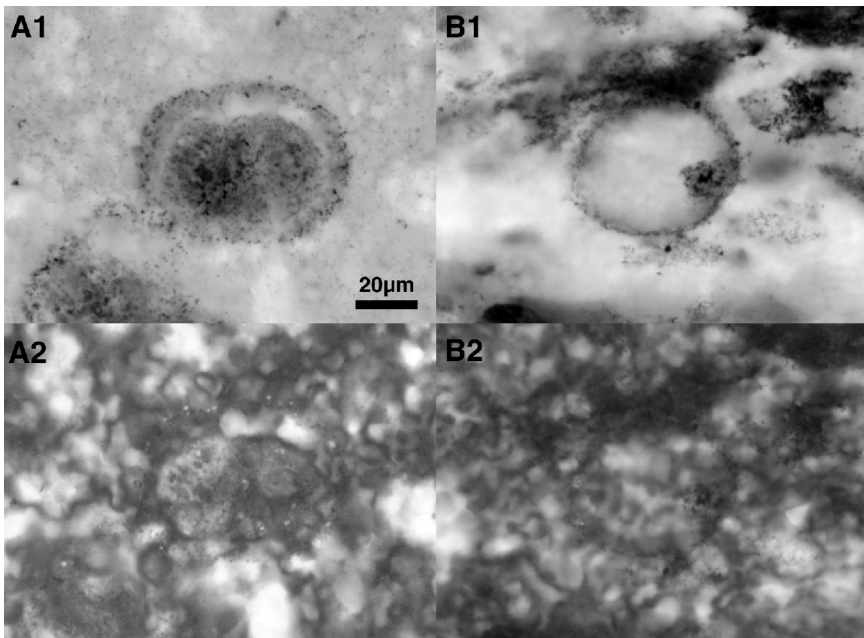


FIG. 5. Photomicrographs in transmitted white light (A1 and B1) and plane-polarized light (A2 and B2), showing relationships between the carbonaceous spheroids and the surrounding matrix minerals (cryptocrystalline quartz). Dark and light particles are carbonaceous materials and carbonates, respectively. See also Figure 4 for their Raman spectra. Scale bar in A1 represents $20\text{ }\mu\text{m}$ for all the figures.

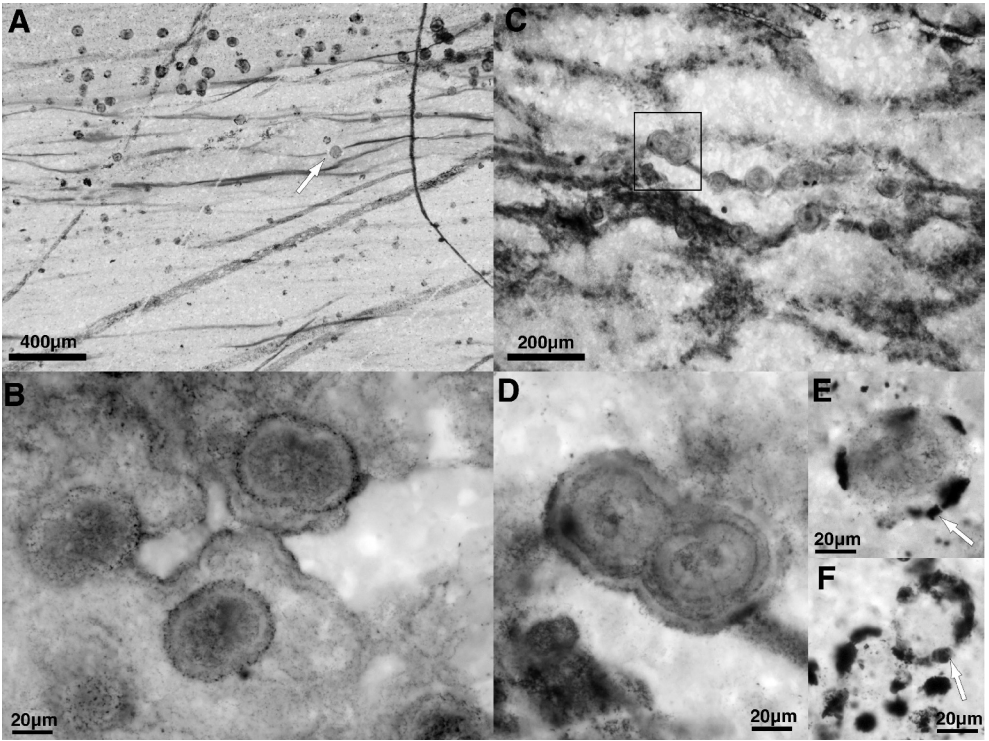


FIG. 6. Photomicrographs showing relationships between the carbonaceous spheroids and sedimentary or diagenetic structures. A, C, and D. Non-compressed spheroids in F5. Arrow indicates the spheroids cutting billowy laminations. Box in C represents area of Figure D. B. Spheroids and rounded thin layers of carbonaceous materials in the F3. E. Altered spheroid partly replaced by pyrite (arrow). F. Altered spheroids replaced by Fe oxide (arrow).

remaining ~25% are single. Exceptionally, several spheroids contain three cell-like units in the outer envelope (Figs. 3AA and 3BB). Some spheroids are squeezed and elongated parallel to the bedding surface (Figs. 2G and 3O). The deformed spheroids exhibit irregular morphologies such as S shapes (Fig. 3O).

Individual cell-like units are spheroidal or hemispheroidal, some of which are crumpled (Figs. 3T and 3V). Paired two cell-like units in most cases have similar diameters. The pair are apparently compressed at attachment (Figs. 3D–3H, 3R, and 3S), although some appear to terminate into another cell-like unit (Fig. 3BB). Some relatively small cell-like units are centrally or excentrally located in the outer envelope (Figs. 3D and 3F). Internal structures of the cell-like units are generally divided into three types: (1) those containing an irregularly shaped, crumpled organic envelope, which typically surrounds a smaller kerogenous mass (Figs. 3H, 3J,

and 3K); (2) those containing a smaller centrally or excentrally located kerogenous mass (Figs. 3L–3M); and (3) those without any kerogenous structure (Figs. 3E, 3G, and 3R).

Size distributions of the measured 460 spheroids are shown in Figure 7. The diameters of the cell-like units range from 4 to 89 μm , and show a bimodal size distribution. Cell-like units of the smaller population are 4 to 22 μm (average 12.6 μm ; $n = 210$), whereas those of larger population are 23 to 43 μm (average 31.4 μm ; $n = 253$), excluding seven exceptionally large specimens (Figs. 3X and 3Y; 47 to 89 μm). The morphologies of the two size populations are almost identical.

Discussion

Two possibilities are considered here for the origin of the carbonaceous spheroids. One is that the spheroids are cellularly preserved microfossils. The

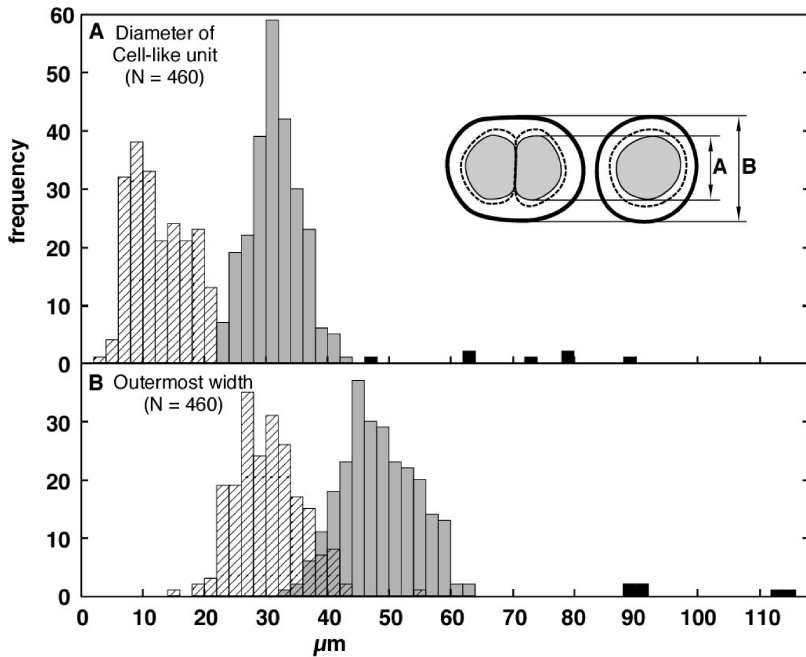


FIG. 7. Size distributions of the carbonaceous spheroids. They are separated into three size populations by their diameters of cell-like units: (1) 4–22 μm (oblique lines); (2) 23–43 μm (grey); and (3) >47 μm (black). Illustration shows the measured dimensions.

morphologies of the spheroids are apparently similar to those of fossilized prokaryotes, especially ensheathed, colonial, coccoid cyanobacteria. Morphologically similar microfossils have been reported from various Proterozoic strata (e.g., Schopf and Blacic, 1971; Hofmann, 1976; Knoll and Golubic, 1979; Nyberg and Schopf, 1984), although not from the Archean so far. The alternative possibility for producing the coccoid-like spheroids is the episodic crystal growth of an inorganic mineral (potentially carbonate and/or silica) during diagenesis. Concentric silica and Fe-oxide microspheres and spherical carbonate micronodules, which are sometimes coated by kerogen, have been reported from several Precambrian cherts (e.g., Klein and Fink, 1976; Awramik et al., 1983; Nyberg and Schopf, 1984). However, criteria distinguishing fossilized coccoid from abiotic spheroids have not been well established. Here, we examine the two contrasting possibilities from the following viewpoints: (1) predominance of paired spheroids; (2) regularity or irregularity of the structures; (3) relationship between organic wall and matrix minerals; (4) relationship between the spheroids and sedimentary

fabrics; (5) size of the cell-like unit; and (6) carbonaceous composition. Some of these characteristics of the Cleaverville spheroids may reflect a microfossil origin, whereas others rather suggest an inorganic origin.

Paired morphologies of the spheroids possibly could have been produced by cell division. On the other hand, nucleation of two nodules in proximity to one another could also produce such paired morphologies inorganically. However, about 75% of the specimens examined are paired rather than single, even in sparsely distributed domains (F1). It is unlikely that the two nucleation sites of mineral growths would so characteristically occur adjacent to one another. If the hypothetical initial precipitates were dumbbell-shaped, the paired spheroids might be preferentially produced inorganically. Recent experiments of crystal growth by Knorre and Krumbein (2000) produced dumbbell-shaped precipitates and paired spherical carbonate nodules. Hence, the paired morphology does not necessarily indicate cell division of fossilized microbes.

Regular concentric morphologies would be easily produced by mineral growth. In contrast,

well-preserved authentic coccoïd microfossils, for example those of ~830 Ma Bitter Springs fossil biota (Schopf, 1968; Schopf and Blacic, 1971; Knoll and Golubic, 1979), tend to show various irregular shapes reflecting cell divisional pattern, mutual compression, post-mortem degradation, and deformation during diagenesis. The Cleaverville spheroids are typically regular and concentric, in which the space between the inner and the outer walls is constant (Figs. 3A–3E, 3G, 3M, 3R–Y, 3AA, and 3BB). These regularities are expected if they are precipitates (Klein and Fink, 1976). However, some Cleaverville spheroids exhibit more irregular morphologies, including a crumpled internal envelope and excentrally located kerogenous mass in the relatively rounded cell-like units (Figs. 3H, 3J–L, 3N, 3P, 3Q, and 3Z), eccentrically located cell-like units in the common envelope (Fig. 3F), and gently deformed outlines such as S-shaped (Fig. 3O), ellipsoidal (Figs. 3J–3K), and irregularly deformed (Fig. 3I) structures. Spherical mineral growth could not simply explain these irregular morphologies. Especially, crumpled internal envelopes in some cell-like units (Figs. 3E, 3G, and 3H) are rather similar to degraded cells of fossilized coccoïds (e.g., Golubic and Hofmann, 1976; Knoll and Golubic, 1979). Even though most spheroids show a regular shape expected for inorganic precipitates, some co-existing ones exhibit more irregular shapes, rather indicating an origin as fossilized cells. In such a case, where these two types occur together, regularity or irregularity in morphology is not critical to assess the origin of the spheroids.

Crystal structures and distributions of surrounding minerals are also helpful to distinguish microfossils from inorganic structures. In the concentric regular-shaped specimens, microcrystalline quartz grains apparently align along the spheroidal morphology, and very fine-grained carbonates occur along organic walls (Fig. 5A). This may suggest that crystal growth produced the structure. On the other hand, non-concentric irregular-shaped specimens are not correlated with the arrangement of the matrix quartz (Fig. 5B). These morphological and mineralogical differences indicate that the two types (i.e., regular-shaped mineralogically controlled spheroid and irregular-shaped ones) are different in origin. However, we still cannot rule out the possibility that the two were the same in origin (either biological or abiological), and partial alteration and/or deformation produced the difference after deposition.

Correlation between the spheroids and sedimentary fabrics is also helpful to distinguish microfossils from diagenetic structures. Some F2 spheroids are compressed parallel to the bedding surface (Fig. 2G) and some are disturbed by stylolites (Fig. 2F). These relations indicate that the deformed spheroids were present before compaction. However, other spheroids appear to have grown over the sedimentary fabric F5 (Figs. 6A, 6C, and 6D). In F5, siliceous lenses and small kerogen clots are elongated, and thus are interpreted to have been compressed. Nevertheless, some spheroids in the same F5 are not compressed (Fig. 6C), suggesting growth after compaction. Further, some spheroids cut the billowy lamination of F5 (Fig. 6A). Therefore, at least some spheroids are not microfossils but represent inorganic structures produced during diagenesis.

The diameters of the cell-like units (4 to 89 μm) are significantly greater than those of typical prokaryotic cells (mostly ~1 μm ; Holt et al., 1994), and are rather similar to those of some cyanobacterial cells. Modern chroococcalean cyanobacteria, such as *Chroococcus turgidus*, are usually 3 to 30 μm in diameter (Holt et al., 1994) and possibly range up to 50 μm (Desikachary, 1959). From this aspect, the Cleaverville spheroids are unusually larger than ordinary prokaryotes, although their large size cannot fully dismiss a microfossil origin.

The carbonaceous compositions of the spheroids could be easily explained by a microfossil origin. On the other hand, spherically grown inorganic minerals (nodules) are not necessarily associated with carbonaceous material. However, organic matter may have coated episodically grown nodule surfaces or be incorporated within nodules (e.g., Buick, 1990). Actually, non-coccoïd-like thin layers of kerogen rarely occur in the F3, which apparently coat botryoidal silica (Fig. 6B), suggesting mobility of the carbonaceous material. This indicates that mineral growth could have produced carbonaceous multi-layers in the chert studied here. Hence, the carbonaceous compositions of the spheroids do not simply indicate a microfossil origin.

Summary

The carbonaceous spheroids from the 3.0 Ga Cleaverville chert morphologically resemble coccoïdal prokaryotes, especially cyanobacteria. Some irregular-shaped specimens appear strikingly similar to degraded prokaryotic cells. Nevertheless,

co-existing regular-shaped concentric spheroids are apparently controlled by mineral growth, some of which have overprinted diagenetic structures. Therefore, at least some spheroids would have been produced by mineral growth during diagenesis. Although biological origin of all the spheroids is not fully dismissed, these observations demonstrate examples of some inorganically produced coccoid-like structures.

Acknowledgments

We thank S. Maruyama, A. Yamagishi, and B. F. Windley for helpful discussions and suggestions. We also thank M. Terabayashi, Y. Kato, H. Ohta, T. Kabashima, and K. Kitajima for great assistance in the field work. Field collaboration with A. Thorne and A. H. Hickman was helpful and much appreciated. Critical comments by S. Awramik and B. Runnegar greatly improved the manuscript. This research was supported by grants from the Ministry of Education, Culture, Sports, Science, and Technology of Japan. YU is grateful for the Research Fellowships of the Japan Society for the Promotion of Science for Young Scientists.

REFERENCES

- Altermann, W., and Kazmierczak, J., 2003, Archean microfossils: A reappraisal of early life on Earth: *Research in Microbiology*, v. 154, p. 611–617.
- Awramik, S. M., Schopf, J. W., and Walter, M. R., 1983, Filamentous fossil bacteria from the Archean of Western Australia: *Precambrian Research*, v. 20, p. 357–374.
- Brasier, M. D., Green, O. R., Jephcoat, A. P., Kleppe, A. K., Van Kranendonk, M., Lindsay, J. F. Steele, A., and Grassineau, N. V., 2002, Questioning the evidence for Earth's oldest fossils: *Nature*, v. 416, p. 76–81.
- Buick, R., 1990, Microfossil recognition in Archean rocks: An appraisal of spheroids and filaments from a 3500 M.Y. old chert-barite unit at North Pole, Western Australia: *Palaios*, v. 5, p. 441–491.
- Cady, S. L., Farmer, J. D., Grotzinger, J. P., Schopf, J. W., and Steele, A., 2003, Morphological biosignatures and the search for life on Mars: *Astrobiology*, v. 3, p. 351–368.
- Desikachary, T. V., 1959, *Cyanophyta*: New Delhi, India, Indian Council of Agricultural Research, 686 p.
- Garcia Ruiz, J. M. et al., 2003, Self-assembled silica-carbonate structures and detection of ancient microfossils: *Science*, v. 302, p. 1194–1197.
- Golubic, S., and Hofmann, H. J., 1976, Comparison of modern and mid-Precambrian Entophysalidaceae (Cyanophyta) in stromatolitic algal mats: Cell division and degradation: *Journal of Paleontology*, v. 50, p. 1074–1082.
- Hickman, A. H., Smithies, R. H., Pike, G., Farrell, T. R., and Beintema, K. A., 2001, Evolution of the West Pilbara granite-greenstone terrane and Mallina Basin, Western Australia—a field guide: *Geological survey of Western Australia Record*, 2001/16, 63 p.
- Hofmann, H. J., 1976, Precambrian microflora, Belcher Islands, Canada: Significance and systematics: *Journal of Paleontology*, v. 50, p. 1040–1073.
- Hofmann, H. J., 2004, Archean microfossils and abiomorphs: *Astrobiology*, v. 4, p. 135–136.
- Holt, J. G., Krieg, N. R., Sneath, P. H. A., Staley, J. T., and Williams, S. T., 1994, *Bergey's manual of determinative bacteriology*, 9th ed. Baltimore, MD: Williams & Wilkins, 787 pp.
- Kato, Y. et al., 1998, Rare earth element variations in mid-Archean banded iron formations: Implications for the chemistry of ocean and continent and plate tectonics: *Geochimica et Cosmochimica Acta*, v. 62, p. 3475–3497.
- Kiyokawa, S., and Taira, A., 1998, The Cleaverville Group in the West Pilbara coastal granitoid-greenstone terrain of Western Australia: An example of a Mid-Archean immature oceanic island-arc succession: *Precambrian Research*, v. 88, p. 109–142.
- Klein, C., and Fink, R. P., 1976, Petrology of the Sokoman Iron Formation in the Howells River Area, at the Western Edge of the Labrador Trough: *Economic Geology*, v. 71, p. 453–487.
- Knoll, A. H., and Barghoorn, E. S., 1977, Archean microfossils showing cell division from the Swaziland system of South Africa: *Science*, v. 198, p. 396–398.
- Knoll, A. H., and Golubic, S., 1979, Anatomy and taphonomy of a Precambrian algal stromatolite: *Precambrian Research*, v. 10, p. 115–151.
- Knorre, H. V., and Krumbein, W. E., 2000, Bacterial calcification, *in* Riding, R. E., and Awramik, S. M., eds., *Microbial sediments*: Berlin, Germany, Springer-Verlag, p. 25–31.
- Nyberg, A. V., and Schopf, J. W., 1984, Microfossils in stromatolitic cherts from the upper Proterozoic Min'yar Formation, southern Ural Mountains, USSR: *Journal of Paleontology*, v. 58, p. 738–772.
- Ohta, H., Maruyama, S., Takahashi, E., and Kato, Y., 1996, Field occurrence, geochemistry, and petrogenesis of the Archean Mid-Oceanic Ridge Basalts (AMORBs) of the Cleaverville area, Pilbara craton, Western Australia: *Lithos*, v. 37, p. 199–221.
- Rasmussen, B., 2000, Filamentous microfossils in a 3,235-million-years-old volcanogenic massive sulphide deposit: *Nature*, v. 405, p. 676–679.
- Schopf, J. W., 1968, Microflora of the Bitter Springs Formation, late Precambrian, central Australia: *Journal of Paleontology*, v. 42, p. 651–688.

- Schopf, J. W., 1993, Microfossils of the Early Archean Apex Chert: New evidence of the antiquity of life: *Science*, v. 260, p. 640–646.
- Schopf, J. W., and Blacic, J. M., 1971, New microorganisms from the Bitter Springs Formation (late Precambrian) of the north-central Amadeus Basin, Australia: *Journal of Paleontology*, v. 45, p. 925–961.
- Schopf, J. W., Kudryavtsev, A. B., Agresti, D. G., Wdowiak, T. J., and Czaja, A. D., 2002, Laser-Raman imagery of Earth's earliest fossils: *Nature*, v. 416, p. 73–76.
- Schopf, J. W., and Oehler, D. Z., 1976, How old are the eukaryotes?: *Science*, v. 193, p. 47–50.
- Sugitani, K., Horiuchi, Y., Adachi, M., and Sugisaki, R., 1996, Anomalously low $\text{Al}_2\text{O}_3/\text{TiO}_2$ values for Archean cherts from the Pilbara Block, Western Australia—possible evidence for extensive chemical weathering on the early Earth: *Precambrian Research*, v. 80, p. 49–76.
- Ueno, Y., Isozaki, Y., Yurimoto, H., and Maruyama, S., 2001, Carbon isotopic signatures of individual Archean microfossils (?) from Western Australia: *International Geology Review*, v. 43, p. 196–212.
- Ueno, Y., Yoshioka, H., Maruyama, S., and Isozaki, Y., 2004, Carbon isotopes and petrography of kerogens in ~3.5-Ga hydrothermal silica dikes in the North Pole area, Western Australia: *Geochimica et Cosmochimica Acta*, v. 68, p. 573–589.
- Walsh, M. M., and Lowe, D. R., 1985, Filamentous microfossils from the 3,500-Myr-old Onverwacht Group, Barberton Mountain Land, South Africa: *Nature*, v. 314, p. 530–532.
- Westall, F. et al., 2001, Early Archean fossil bacteria and biofilms in hydrothermally-influenced sediments from the Barberton greenstone belt, South Africa: *Precambrian Research*, v. 106, p. 93–116.